Biosensors and Bioelectronics 131 (2019) 287–298

Contents lists available at ScienceDirect

Biosensors and Bioelectronics

journal homepage: www.elsevier.com/locate/bios

Electrochemical cardiovascular platforms: Current state of the art and beyond

Sabine Szunerits[a,*], Vladyslav Mishyn[a], Iwona Grabowska[b], Rabah Boukherroub[a,*]

[a] Univ. Lille, CNRS, Centrale Lille, ISEN, Univ. Valenciennes, UMR 8520-IEMN, F-59000 Lille, France
[b] Institute of Animal Reproduction and Food Research, Polish Academy of Sciences, Tuwima 10, 10-748 Olsztyn, Poland

ARTICLE INFO

Keywords:
Cardiac biomarkers
Immunosensors
Electrochemistry
Aptamers

ABSTRACT

Cardiovascular diseases (CVD) remain the leading cause of death within industrialized nations as well as an increasing cause of mortality and morbidity in many developing countries. Smoking, alcohol consumption and increased level of blood cholesterol are the main CVD risk factors. Other factors, such as the prevalence of overweight/obesity and diabetes, have increased considerably in recent decades and are indirect causes of CVD. Among CVDs, the acute coronary syndrome (ACS) represents the most common cause of emergency hospital admission. Since the prognosis of ACS is directly associated with timely initiation of revascularization, missed, misdiagnosis or late diagnosis have unfavorable medical implications. Early ACS diagnosis can reduce complications and risk of recurrence, finally decreasing the economic burden posed on the health care system as a whole. To decrease the risk of ACS and related CVDs and to reduce associated costs to healthcare systems, a fast management of patients with chest pain has become crucial and urgent. Despite great efforts, biochemical diagnostic approaches of CVDs remain difficult and controversial medical challenges as cardiac biomarkers should be rapidly released into the blood at the time of ischemia and persistent for a sufficient length of time to allow diagnostics, with tests that should be rapid, easy to perform and relatively inexpensive. Early biomarker assessments have involved testing for the total enzyme activity of aspartate aminotransferase (AST), lactate dehydrogenase (LDH) and creatine kinase (CK), which cardiac troponins being the main accepted biomarkers for diagnosing myocardial injury and acute myocardial infarction (AMI).

To allow rapid diagnosis, it is necessary to replace the traditional biochemical assays by cardiac biosensor platforms. Among the numerous of possibilities existing today, electrochemical biosensors are important players as they have many of the required characteristics for point-of-care tests. Electrochemical based cardiac biosensors are highly adapted for monitoring the onset and progress of cardiovascular diseases in a fast and accurate manner, while being cheap and scalable devices. This review outlines the state of the art in the development of cardiac electrochemical sensors for the detection of different cardiac biomarkers ranging from troponin to BNP, N-terminal proBNP, and others.

1. Introduction

Cardiovascular diseases, ranging from coronary heart disease to heart failure, are major emergent health problems (Fig. 1). They are a result of cardiac overload or injury and are outcomes from different changes acting on the cardiac interstitium and/or cardiac myocytes. Coronary heart disease is probably the most common form among the different cardiovascular diseases occurring when the arteries supplying blood to the heart narrow or harden. One of the life threatening forms of acute coronary syndromes (ACS) is acute myocardial infarction (AMI), known more commonly as heart attack due to the sudden occlusion of a coronary artery by thrombus or by embolization. As AMI can cause irreversible heart damage and can ultimately lead to heart failure, early and fast diagnosis of possible AMI is of paramount importance to prevent and attenuate its progression.

The existing clinical methodologies to detect heart diseases are based, next to physical examination, on electrocardiograms (ECG), electrocardiography chest X-rays, and echocardiograms (Fig. 2). These approaches are equipment dependent as well as time-consuming and expensive. The results of these methods proved to be not entirely reliable to diagnose cardiac vascular diseases; up to 70% of patients demonstrated normal ECG readings upon hospital admission related to acute coronary syndromes (Morrow et al., 2007).

Enzyme-linked immunosorbent assays (ELISA) remain the golden

* Corresponding authors.
E-mail addresses: Sabine.szunerits@univ-lille.fr (S. Szunerits), rabah.boukherroub@univ-lille.fr (R. Boukherroub).

https://doi.org/10.1016/j.bios.2019.02.010
Received 3 December 2018; Received in revised form 18 January 2019; Accepted 4 February 2019
Available online 19 February 2019
0956-5663/

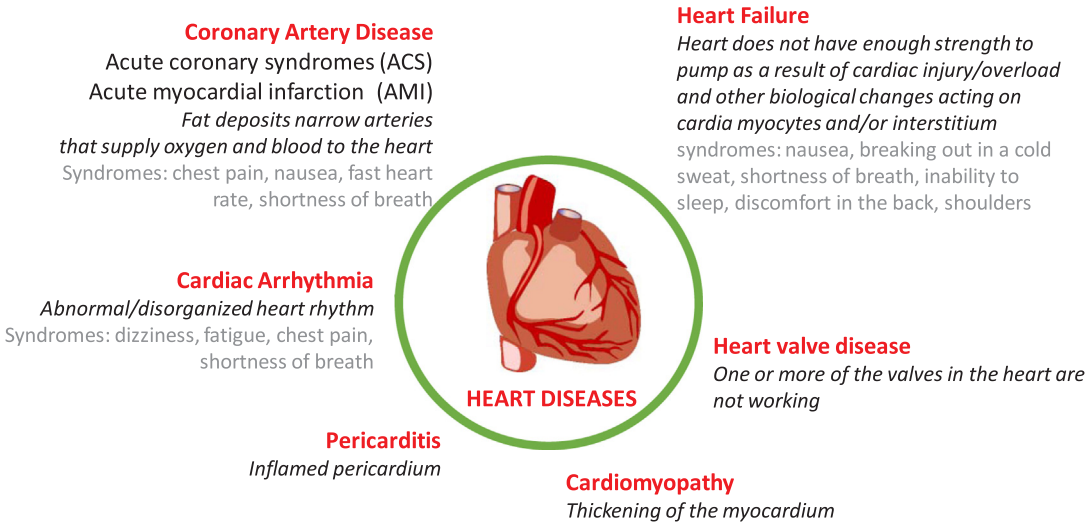

Fig. 1. Classification of cardiovascular diseases.

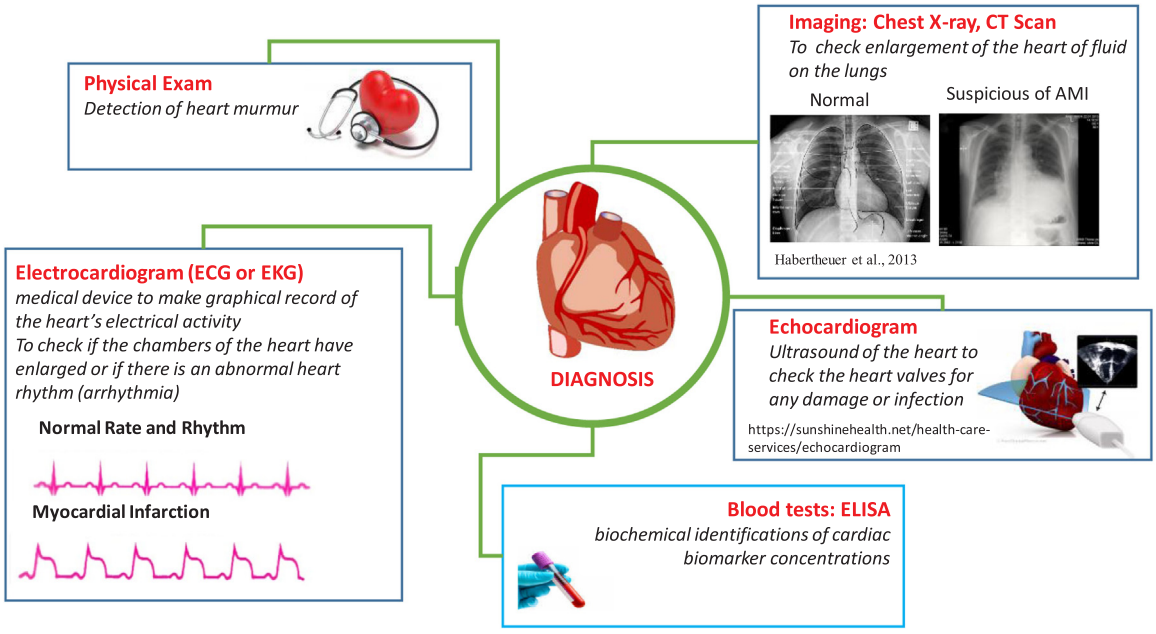

Fig. 2. Current diagnostic tools to detect cardiovascular diseases in clinical settings.

standard in clinical settings to analyze blood samples from patients with suspicion for cardiovascular diseases. Cardiac biomarkers are protein molecules which are released into the blood stream in the case of heart muscle damage with a characteristic rise and fall pattern (Fig. 3**A**). In particular, the levels of cardiac troponins, such as cTnI and cTnT, have found to have a significant correlation with the onset of acute myocardial infarction (AMI) and is one of the most widely used biomarkers for this disease (Table 1) and has resulted in the development of the first bedsit troponin testing methods (Hamm et al., 1997).

Despite the well acceptance of the ELISA kits in clinical settings due to the accuracy of the technique providing trustworthy results for a variety of different cardiac biomarkers, ELISA tests are time consuming, expensive and in several cases not adapted with the requested clinical cut-off levels. Recognized guidelines recommend an analysis time of less than one hour, once the patient is admitted to the hospital (Apple et al., 2007). The development of immunosensors, generating a specific analytical signal upon the interaction of cardiac biomarkers with an antibody modified surface, meets these challenges and enormous research has been put into the development of portable and fully automated cardiac point-of care sensors with analysis time within max 20 min. The sensing strategies behind cardiac immunosensors together with their advantages and limitations will be outlined in this review. A main breakthrough came with the electrochemical based troponin sensing device by Abbott Point of care, the i-STAT sensor. A special focus will be therefore devoted to electrochemical sensing platforms believed to meet all the future demands such as sensor miniaturization, high sensitivity and selectively in a label-free detection process, short detection times and the possible for developing wearable and implantable sensor technologies to overcome the current limitations of ELISA platforms.

2. History of cardiac biomarkers

One of the first biomarkers used in the diagnosis of acute myocardial infarction (AMI), Aspartate Transaminase (AST), was even incorporated into the World Health Organization (WHO) definition of AMI in the 1960s(Ladue et al., 1954). However, as it was found later that AST is not specific for cardiac muscle alteration, and its detection

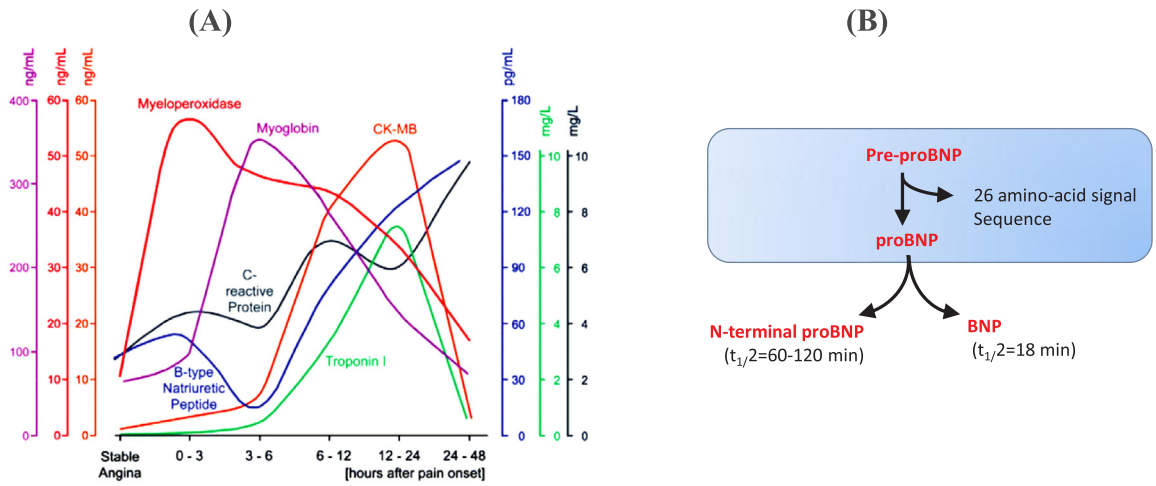

Fig. 3. (A) Time-dependent concentration profile in biomarker concentration after chest pain onset (reprint with permission from Ref. Sinning et al. (2008); (B) Biological pathway of natriuretic peptides leading to the production of NT-proBNP and BNP biomarkers.

Table 1
Different identified cardiac biomarkers.

Cardiac biomarker	*Cardiovascular disease indicator*	*Cut-off level*	*References*
Creatine kinase-MB *(CK-MB)*	Early detection of myocardial infarction, moderate specificity (also released following skeletal muscular injury)	10 ng mL^{-1}	(Sinning et al., 2008)
Troponin I *(cTnI)*	Detection of myocardial infarction Highly specific	0.03 ng mL^{-1}	(Hamm et al., 1997)
Troponin T *(cTnT)*	Detection of myocardial infarction Highly specific	0.01 ng mL^{-1}	(Hamm et al., 1997)
Myoglobin	Early detection of myocardial infarction, low specificity (also released following skeletal muscle injury), rapid clearance	70–200 ng mL^{-1}	(Sinning et al., 2008)
Lipoprotein-associated phospholipase A2 *(Lp-PLA_2)*	Marker of inflammation risk predictor for stroke	> 200 ng mL^{-1}	(Colley et al., 2011)
Interleukin-6 *(IL-6)*	Precocious biomarker of inflammation associated with increased incidence of myocardial infarction	> 1 pg mL^{-1}	(Wainstein et al., 2017)
Interleukin-1 *(IL-1)*	Promotes the formation of the atherosclerotic plaque		(Buckley and Abbate, 2018)
Low-density lipoprotein *(LDL)*	Cause plaque formation, casual factor in the pathophysiology of CVD	> 160 mg dL^{-1}	(Ference et al., 2017)
Myeloperoxidase *(MPO)*	Detection of inflammation Moderate specificity	> 350 ng mL^{-1}	(Sinning et al., 2008)
TnF-alpha	Inflammation, cardiac risk factor Low specificity	> 3.6 pg mL^{-1}	
Brain-type natriuretic peptide *(BNP)*	Indication of acute coronary syndrome, diagnosis of heart failure, or ventricular overload, highly specific, short life time	0.1 ng mL^{-1}	(Palazzuoli et al., 2010)
N-terminal BNP *(NT-proBNP)*	Highly linked to acute heart failure indication of ischemia or necrosis	0.25–2 ng mL^{-1}	(Horii et al., 2013)
C-reactive proteins *(CRP)*	Highly specific for ischemic events Moderate specificity	< 1 μg mL^{-1} (low risk) > 3 μg mL^{-1} (high risk)	(Sinning et al., 2008)
Heart fatty acid binding protein *(H-FABP)*	Myocardial necrosis Low specificity	> 6 ng mL^{-1}	(Otaki et al., 2017)

is, therefore, not specific for cardiac damage, by 1970s, two further cardiac biomarkers were in use: lactate dehydrogenase (LDH) and creatine kinase (CK). (Panteghini, 1995) (Table 1). LDH and its co-enzyme LDH-1 increases in blood 5–10 h after AMI and reaches a maximum value in the blood in 60–144 h before returning to the normal level in 12 days. (Penttila et al., 2000). CK is more specific than LDH in the context of AMI, especially in patients having other co-morbidities such as muscle or hepatic disease (Danese and Montagnana, 2016). While the total CK activity may be indeed related to the extend of myocardial infractions, this biomarker is characterized by low specificity, since its activity increases considerably in liver, kidneys an skeletal muscle diseases.

In humans, the enzyme CK is present in three isoenzymes CK-MM, CK-BB and CK-MB, the same originating from the various combinations of the muscle (M) and brain (B) isoforms. While CK-BB is rarely present in the bloodstream, the myocardium has 70% of CK-MM and 30% of CK-MB. Several studies confirmed that CK-MB provides a reliable and specific diagnosis in the first hours of cardiac symptoms (Table 1). CK-MB, used for the detection of myocardial infarction and re-infarctions, rises 4–6 h after infraction onset with a maximum value about 12 h thereafter. However, CK-MB activity is influenced by several analytical variables such as assay temperature, and pH. Moreover, the activity of CK-MB is also enhanced in many skeletal muscle disorders, as well as in the case of cocaine abuse which resulted in further research aimed to identify a more reliable biomarker.

Myoglobin, a small globular oxygen-carrying protein, which concentration rises after AMI, has been proposed in 1978 as a cardiac biomarker. It is freed within 1 h from tissue damage, peaks after 6–9 h and returns to normal levels (17.4–105.7 ng mL^{-1}) after 1 day (Fig. 3**A**). However, because of rapid clearance from blood, myoglobin may

"miss" late-presenting patients. Myoglobin levels are likewise increased in the case of renal failure, inflammatory myopathies, shock and trauma, and elevated myoglobin levels do not necessarily mean myocardial injury.

The cardiac biomarkers with high specificity for AMI are cardiac troponins (cTn) such as cTnI and cTnT, with a half-life time of 2–4 h. In particular, cTnI sensing has become the golden standard myocardial infarction diagnosis, owing to its production only in the case of direct damage of the myocardium. Indeed, cTnT is reported to be also elevated in patients with chronic renal failure. Troponin levels rise 2–3 h after myocardial injury onset and persist for 10 days thereafter (Fig. 3**A**).

Another class of cardiac biomarkers are natriuretic peptides, regulatory diuretic-natriuretic substances responsible for lowering blood pressure. One of the most important biomarkers for heart failure are brain-type natriuretic peptides (BNP) and *N*-terminal proBNP (NT-proBNP). High levels of NT-proBNP have been associated with cardioembolic strokes due to atrial fibrillation and are used to predict the development of atrial fibrillation. It acts as a predictor of mortality after stroke. BNP is synthesized by the heart ventricles and released under heart stress situations. It is synthesized as pre-proBNP, which is converted to proBNP and cleaved to produce BNP and NT-proBNP (Fig. 3**B**). While BNP has a half-life of only 20 min and is quickly cleared, NT-proBNP circulates for 1–2 h leading to higher circulation levels and lower fluctuations.

Nevertheless, BNP would be the more desirable biomarker for heart failure due to its fast release kinetics and well defined cutoff level of 100 pg mL^{-1} (Table 1). Due to their difference in metabolism, plasma levels of NT-proBNP are also more influenced by renal function (Horii et al., 2013) and are strongly susceptible to the age of the patient. The detection of BNP is challenging compared to other cardiovascular biomarkers, as the blood BNP level under normal conditions is low (20 pg mL^{-1}; 6 pM) and rises to only about 2 ng mL^{-1} (600 pM) in patients with acute heart failure (Palazzuoli et al., 2010).

C-reactive protein (CRP) has to be added to the list of validated cardiac biomarkers. It is an acute-phase protein with plasma levels increasing up to 10.000 times its normal level upon ischemic events, characterized by a limited blood flow to the brain, which leads to the death of brain tissue, cerebral infarction, and, in the worth case, to ischemic stroke.

Some other biomarkers have been added to the list of cardiac biomarkers such as myeloperoxidase (MPO), TnF-alpha, or the heart fatty acid binding protein (H-FABP) (Table 1). Their specificity to heart diseases is currently less understood and are thus only limited for assay development with no sensor for these biomarkers commercialized up to now.

3. Immunosensors for cardiac biomarkers

3.1. Antibody based sensors

Most of the current reported cardiac biosensors are affinity sensors. Like ELISA assays, the detection of the target is a result of a specific binding of the analyte antigen to the particular region of the antibody attached to the transducer surface (Fig. 4). As the binding constant between antigen and antibody is very large, such systems are only reversible under certain conditions. While a larger range of surface chemistry strategies could be employed to link cardiac antibodies to sensing transducer, surface attachment is achieved almost exclusively until now via amide coupling chemistry (Fig. 4). Carboxylic acid functions can be easily introduced onto gold interface using molecules such as mercaptoundecanoic acid, dithiobis(succinimidyl propionate) or 3, 3'-dithiobis (sulfosuccinimidyl propionate). These linkers bear thiol groups at one end, promoting binding to the gold interface, and carboxylic or ester bonds at the other end for covalently linking of the cardiac antibody. Other linkers such as 3-aminopropyltriethoxysilane (APTS) or diazonium salts (Serafin et al., 2018) are used according to the substrate and the material of the transducer interface.

For a highly sensitive immunosensor, an optimal ligand-spacer ratio exists and has to be experimentally determined. There is much freedom over the assay type used and a wealth of cardiac biosensor concepts exist (Fig. 4). The omission of a secondary incubation reduced the complexity of the sensor construction, reduced costs per assay as antibodies and labels contribute to the cost of the assay. These benefits of label free cardiac sensors are however often offset by a lower and not adequate detection limit, limiting the implementation into clinical setting. The sandwich assay remains the most widely employed strategy consisting of a cardiac antibody modified substrate, complementary to the cardiac biomarkers. This step is a means of spreading the sample target biomarker during the incubation step. Upon completion of the binding, a secondary antibody is introduced containing a label complementary to the free epitope on the now captured cardiac biomarker. In this configuration, the target biomarker is essentially sandwiched between the two reaction antibodies, resulting in increased sensitivity. The analyte concentration is determined by estimating the amount of enzyme activity produced when an enzyme specific substrate is added. Enzymatic labels such as horseradish peroxidase (HRP) (Azevedo et al., 2003) are widely investigated.

Apart from HRP, fluorescent labels (Acharya et al., 2013) are widely used and are the base of most marketed cardiac assays. Although fluorescence-based immunosensors achieve high sensitivity, their drawback is their tedious labeling process and control of the amount of fluorophore on each molecule, important for making quantitative analysis possible.

3.2. Aptamer based cardiac biosensors

Unlike protein antibodies, DNA aptamers are quickly synthesized in large quantities and represent a new way to detect cardiac protein biomarkers (Chekin et al., 2018; Grabowska et al., 2018). Some of the reported cardiac aptamers are listed in Table 2. The DNA sequence was obtained by the SELEX method. After several selection and amplification steps, the most specific sequence was tested for its binding affinity and dissociation constant (K_d) to the targeted cardiac biomarker using surface plasmon resonance (SPR) or other affinity based methods such as fluorometry. The sequences reported below have been chosen based on their highest affinity to the biomarkers (usually from pM to mM range) and hold a promising role in scope to substitute commonly used antibody transducers in biosensing. For the cTnI, Tro4 aptamer is the best choice (Jo et al., 2015). This aptamer has a binding affinity constant towards cTnI of 270 pM with a structure as predicted in Fig. 5**A**. Wang et al. (2015) using the SELEX process selection proposed a highly selective BNP aptamer for BNP-32 peptides (Fig. 5) with a dissociation constant $K_d = 12 \pm 0.1$ nM.

In contrast to antibodies, where surface attachment is done almost exclusively via amide coupling, in the case of aptamers, several surface attachment strategies have been proposed. Indeed, different surface functions (e.g. thiol, azide, propargyl, etc.) can be easily incorporated into the aptamer. We have demonstrated lately that next to amide coupling (Fig. 5**A**) between the 5'-NH_2 group and the thymine nucleotide of the aptamer to the surface linked carboxylic acid functions (Chekin et al., 2018), surfaces bearing propargyl function can be modified via "click" chemistry with aptamer ligands carrying azide function (Fig. 5**B**) (Grabowska et al., 2018).

A main concern is the possibility of background interference due to nonspecific adsorption of other molecules. Like in other sensing technologies, anti-fouling molecules such as poly(ethylene) glycol derivatives, serum molecules, etc. need to be in addition linked to the surface of the sensor to circumventing non-specific interactions and to limit non-specific signal (Chekin et al., 2018).

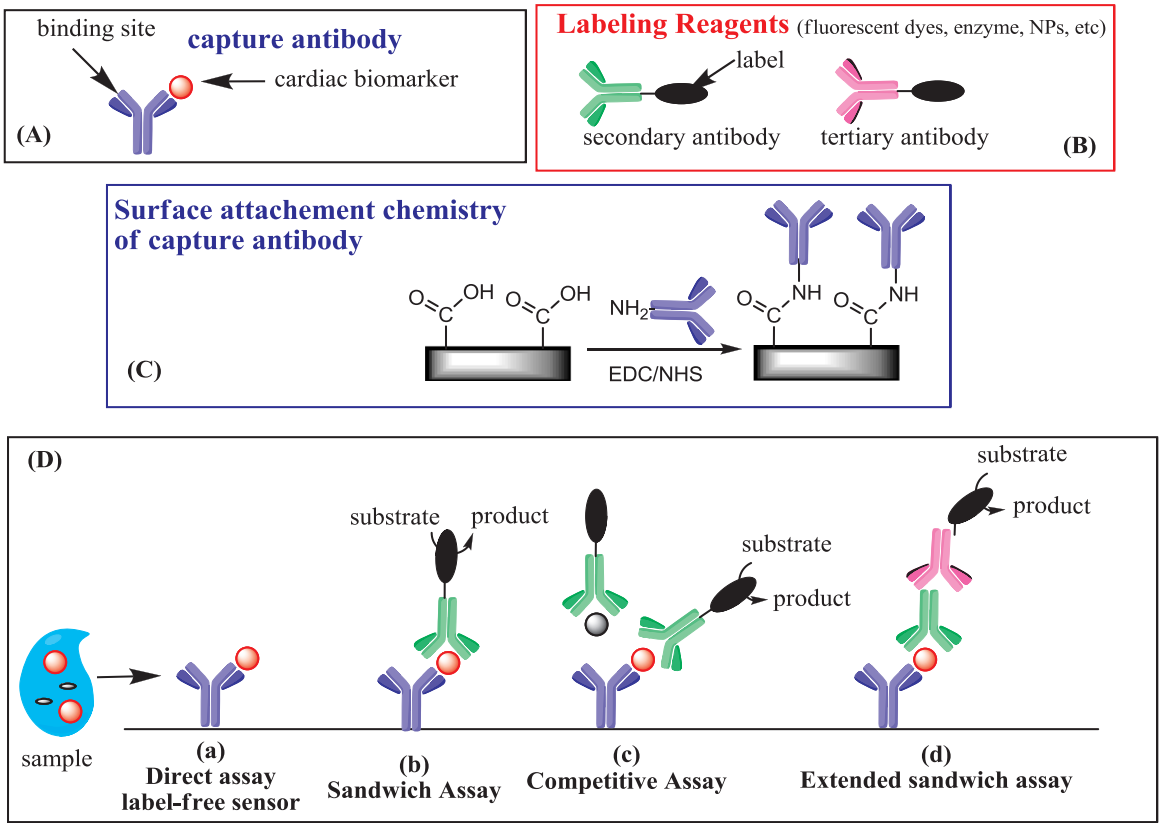

Fig. 4. Progressive interaction steps leading to the final binding structures D. (A) Binding of cardiac biomarker to capture antibody; (B) Labeling of antibodies; (C) Surface attachment chemistry to link antibody to transducer; (D) Different possible immunoassay binding configurations used in the development of cardiac biosensors: (a) the direct, label-free concept where a surface immobilized antibody is used to capture the cardiac biomarker antigen and the binding event results in a detectable signal change; (b) Sandwich structure formation using labeled secondary antibodies for detection; (c) Competitive immunoassays using labeled antibodies/antigens; (d) Extended sandwich assay using a tertiary antibody for sensing.

4. Cardiac biomarkers sensing methodologies

Next to the choice of the right surface ligand and surface attachment chemistry, the biosensor signal dictates the final structure of the resulting diagnostic device. The transducer has to be chosen correctly to allow minimally invasive, rapid and highly sensitive cardiac biomarker detection. Given the wide interest in cardiac immunosensors, several detection methodologies have been implemented (Table 3).

4.1. Optical techniques

Within clinical settings, the most common way for detecting a cardiac immunoreaction event is by optical means (Fig. 6). These include a broad spectrum approaches such as fluorescence intensity measurements, luminescence generating immunoassays, surface plasmon resonance (SPR) based sensing, localized surface plasmon resonance (LSPR) as well as metal-enhanced fluorescence sensing and more recently surface-enhanced Raman spectroscopy. Wu et al. (2010)

Table 2
DNA sequences for cardiac aptamers together with the dissociation constant for the corresponding biomarker.

Biomarker	*Aptamer-sequence 5′→3′*	K_d	*References*
cTnI	CGT GCA GTA CGC CAA CCT TTC TCA TGC GCT GCC CCT CTT A	270 pM	(Jo et al., 2015)
	GCC TGT TGT GAG CCT CCT AAC TAC ATG TTC TCA GGG TTG AGG CTG GAT GGC GAT GGT GGC ATG CTT ATT CTT GTC TCC C	9.009 ± 2.437 nM	(Dorraj et al., 2015)
cTnT	CGT AGA ATT CAT GAG GAC GTT ACG TAC CGA CTT CGT ATG CCA ACA GCC CTT TAT CCA CCT CAG CTA AGC TTA CCA GTG CGA T	43.8 ± 13.7 nM	(Ara et al., 2012)
BNP	GGC GAT TCG TGA TCT CTG CTC TCG GTT TCG CGT TCG TTC G	12 nM	(Wang et al., 2015)
	ATA CGG GAG CCA ACA CCA CGT TGC GCA GCT GGG GGC AGT GCT CTT TCG ATT TGG AGA GCA GGT GTG ACG GAT	N/A	(Bruno et al., 2014)
	TAA ACG CTC AAA GGA CAG AGG GTG CGT AGG AAG GGT ATT CGA CAG GAG GCT CAC A	N/A	(Lin et al., 2009)
Myoglobin	GAC AGG CAG GAC ACC GTA ACC CC TCC TTT CCT TCG ACG TAG ATC TGC TGC GTT GTT CCG ACT GCT ACC TCC CTC CTC TTC	4.93 nM	(Wang et al., 2014)
CK-MB	GGG GGG TGG GTG GGG GAT CTC GGA GGA TGC TTT TAG GGG GTT GG	0.81 ± 0.79 nM	(D. Zhang et al., 2018; J. Zhang et al., 2018)
	CAC CTA ATA CGA CTC ACT ATA GCG GAT CCG AAA GTC GGA GCA GAA GTT GCC TCA TAG CTG GGA AAC CTG CCC TGG CTC GAA CAA GCT TGC	43 mM	(Kim, 2015)
NT-proBNP	CAC CTA ATA CGA CTC ACT ATA GCG GAT CCG ATA GGG TTG TAC TTT CGA TAG CCA GGG CTT GGG GTG GTT GGC TGG CTC GAA CAA GCT TGC	55 nM	(Kim, 2015)
CRP	CGA AGG GGA TTC GAG GGG TGA TTG CGT GCT CCA TTT GGT G	16.2 nM	(Wu et al., 2016)

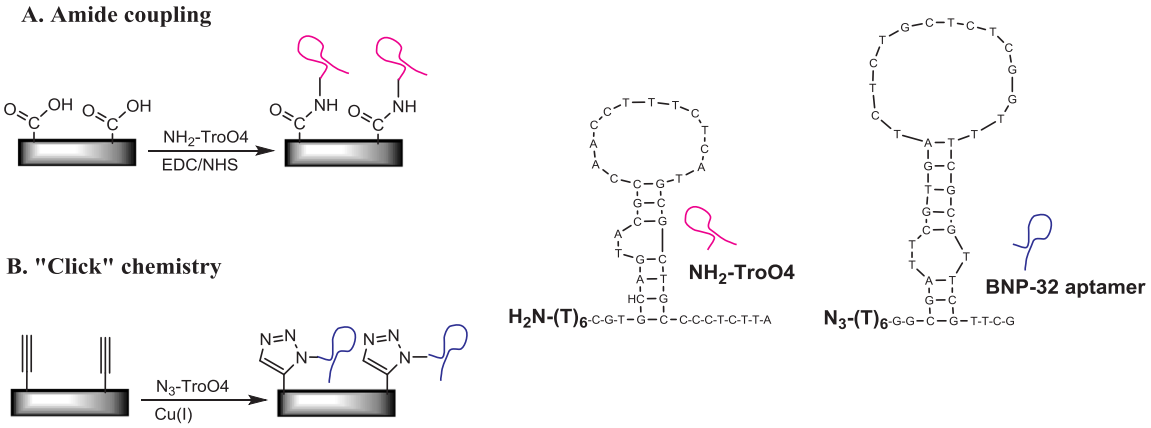

Fig. 5. Ilustration of the construction of an immunosensor: (A) Amide coupling for the generation of a sensor specific for cTnI proteins (MW = 24 kDa); (B) Use of "click" chemistry for the integration of a BNP-32 aptamer for the sensing of BNP-32 peptide (MW = 3.4 kDa).

proposed a colorimetric sensor for cTnI based on a poly(dimethylsiloxane (PDMS))-gold composite interface (Fig. 6**A**). The ability of gold nanoparticles (AuNPs) to be functionalized with cardiac antibodies makes them ideal cardiac sensing substrates. The colorimetric technique has the advantage of being easy to perform, with its drawbacks including difficult labeling procedure as well as bulky sensing instrumentation. An innovative fluorescence based sensor is that reported by Kar et al. (2012) using TiO_2 nanotubes for cTnI sensing (Fig. 6**B**). While an impressive low detection limit for cTnI was achieved with this sensor, the major disadvantage lies in the tedious labeling process.

Surface plasmon immunosensing technology has been recently successfully applied by Pawula et al. (2016) (Fig. 6**C**). In the label-free direct assay mode, a detection limit of 5 ng mL^{-1} for cTnI was achieved, which could be lowered to 500 pg mL^{-1} using Au NPs functionalized antibodies as amplification. The sensor proved to give a rapid response in real-time and the interface can be reused for multiple sample analysis. However, the detection limits are far beyond current cut-off levels for cTnI. Using carboxymethyldextran-modified SPR sensors, the detection limit of cTnI could be lowered to 10 pg mL^{-1} (Dutra and Kubota, 2007). A paramagnetic immunoassay, based on the combination of magnetic nanoparticles and an optical read out, allowed for a rapid and highly sensitive detection of cTnI with a LOD of 30 pg mL^{-1} cTnI (Bruls et al., 2009) (Fig. 6**D**).

A well performing localized surface plasmon resonance platform using triangular gold nanoprisms modified with anti-cTnI is that of Liyanage et al. (2017). The cTnI biosensors were prepared using self-assembled monolayers having different alkyl spacer lengths. As expected, the sensor prepared with 6-mercaptohexanoic acid (MHNA) /1-hexanethiol (HT) provides the shortest distance between the gold nanotriangles and the biomarkers and produced the lowest detection limit. One of the drawback of LSPR is the low penetration length (100 nm) into the sensing medium, making the detection of larger biomolecules difficult and reducing the sensing ability in complex solution such as blood. Tadepalli et al. (2015) investigated short peptides as biorecognition elements instead of larger antibodies to overcome this limitation in LSPR sensing (Fig. 6**E**). Chon et al. (2014) reported lately on the possibility of using SERS-based competitive immunoassays for troponin I and CK-MB detection. With a LOD of 33.7 pg mL^{-1} for cTnI, the interface is adapted for current cTnI sensing.

Lateral flow assays (LFA) based on immunostrips and colloidal particles is a widely used sensing technology due to its simple operation mode. Lately the low sensitivity of LFA could be overcome through the combination with core-shell surface-enhanced Raman spectroscopy (SERS) tags and used for early diagnosis of AMI (Fig. 6**F**) (D. Zhang et al., 2018; J. Zhang et al., 2018b). Due to the amplified signal of the SERS nanotags, a detection limit of three cardiac biomarkers, Myo, cTnI, CK-MB, down to 1, 0.8 and 0.7 ng mL^{-1} respectively was achieved.

4.2. Electrochemical and electrical techniques

Next to the optical techniques, electrochemical biosensors are prominent players (Bunyakul and Baeumner, 2015; Kaisti, 2017) for clinical analysis and have received great attention with a wealth of publications and demonstrations of unique detection platforms.

Table 3
Technologies used for cardiac biomarkers sensing.

Technology	*Advantages*	*Disadvantages*
Optical detection		
Fluorescence intensity measurement	High sensitivity	Need of fluorescent labeling Bulky sensing instrumentation
Colorimetric sensing	Easy to perform	Need for enzymatic labels Bulky sensing instrumentation
Luminescence generating assays	Easy detection	Need for enzymatic labels
Surface plasmon resonance (SPR	Label-free	Bulky instrumentation Limited sensitivity without label
Localized surface plasmon resonance (LSPR)	Label-free	Low penetration length reducing the sensing in complex solutions such as blood.
Surface enhanced Raman spectroscopy (SERS)	Multiplexing	Limited sensitivity Bulky instrumentation
Electrochemical detection		
Amperometric	Commercial sensor Easy to perform	Limited sensitivity without using secondary antibodies with enzymatic or other chemical labels
Impedimetric	Label-free	Limited sensitivity
Potentiometric (Field Effect Transistor)	Label-free Miniaturisable, flexible	Complex fabrication process

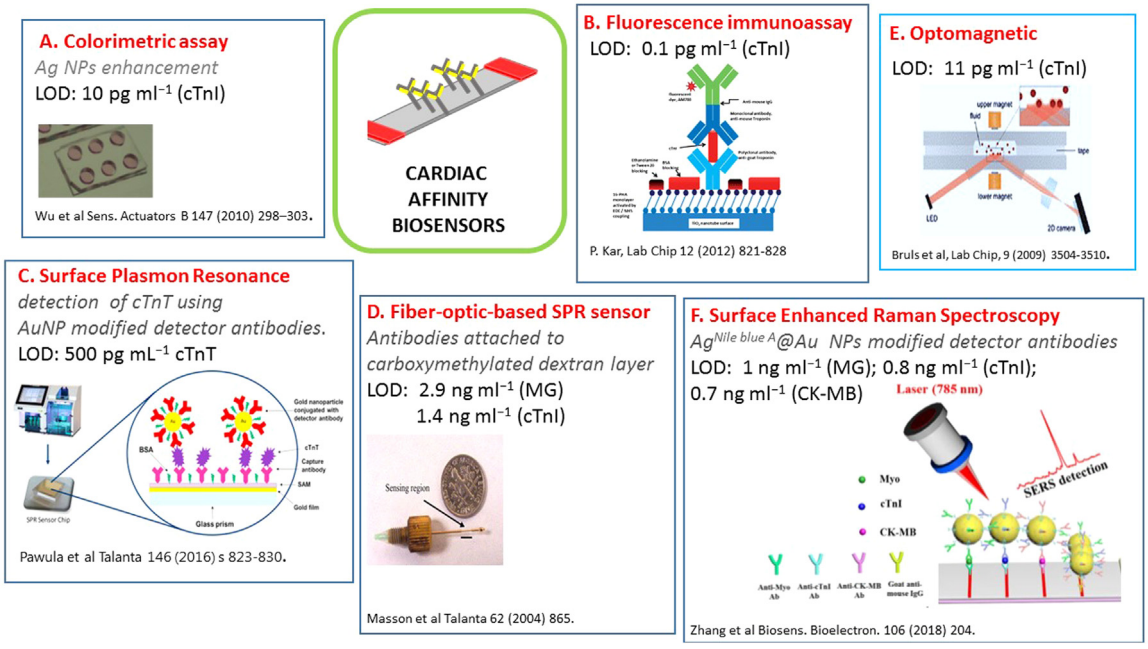

Fig. 6. Different affinity biosensors for the detection of cardiac biomarkers using optical read out strategies: (A) colorimetric assay using Ag NPs enhanced read out (Wu et al., 2010); (B) Fluorescence based sensing using a fluorescence labeled tertiary detection antibody (Kar et al., 2012), (C) SPR based sensors using carboxymethyldextran-modified SPR sensors, (Pawula et al., 2016), (D) Fiber-optic based SPR sensor (Masson et al., 2004), (E) Optomagnetic sensor (Bruls et al., 2009) based cTnI sensor, (F) Illustration of SERS detection using core-shell SERS nanotag-based LFA (reprint with permission from D. Zhang et al. (2018)).

Electrochemical sensors are classified depending on the detection principle and one can distinguish impedimetric, amperometric, potentiometric and conductance-based sensors (Fig. 7). These sensors operate on the principle of change in the current, impedance or potential when an immunoreaction takes place on the surface of the electrode of the sensor. The advantages of electrochemical sensors are their robustness and real time detection. These analytical platforms require cheap instrumentation, and have shown to provide low detection limits upon optimization. The possibility for miniaturization offers in addition many of the desirable attributes for point-of-care tests. Electrical biosensors overcome the limitations of colorimetric and fluorescence immunoassays and result in high sensitivity. However, their detection environment such as solution pH and ionic strength can perturb the sensing results.

The best known example is the i-STAT electrochemical sensor marked by Abbott Point of Care. It is a whole blood amperometric based sandwich immunosensing device, capable of measuring the concentrations of different cardiac biomakers. Antibodies specific for the different analytes are located on the electrochemical sensor fabricated on a silicon chip. Deposited on another location of the sensor is the alkaline phosphatase enzyme labeled secondary antibody conjugate specific to a separate portion of the analyte molecule.

A multiplexed configuration for NT-proBNP and CRP sensing was lately proposed (Fig. 7**A**) (De Avila et al., 2014). Carboxylic acid-modified magnetic beads were modified with NT-proBNP and CRP specific capture antibodies and the quantification was performed by an indirect competitive as well as sandwich-type immunoassay, respectively, using HRP-labeled tracer. The method allowed matching the clinically relevant concentration ranges for both cardiac biomarkers using the same electrode platform, and the whole multiplexed immunoassay could be completed in 1 h approximately.

Some of the electrochemical methods are label-free approaches such as Electrochemical Impedance spectroscopy (EIS); they play a momentous role in the label-free analysis of biomarkers (Table 4). Impedimetric sensors measure changes in the impedance values when a potential is applied to the electrode, immersed in an electrolyte. The formed electrical double layer is modulated when cardiac biomarkers bind to surface immobilized antibodies. One example is the zinc oxide (ZnO) nanosensor by Shanmugam et al. for the detection of cTnT and cTnI (Fig. 7**B**) (Shanmugam et al., 2016, 2017). It is an immunological assay involving the binding of cTnI and cTnT antibodies to ZnO nanorods deposited on a flexible substrate modified with a thiol linker where cTnI and cTnT can be detected in a label-free manner by EIS in the 1 pg mL^{-1} range in human serum (Shanmugam et al., 2017).

Another electrochemical technique widely employed is differential pulse voltammetry (DPV) (Fig. 7**C**). We demonstrated recently the utility of nitrogen-doped reduced graphene oxide (N-prGO) for quantifying cTnI. N-prGO was functionalized with 1-pyrenecarboxylic acid and poly(ethylene glycol) pyrene ligands to which Tro4 aptamers were integrated. Using DPV and $[Fe(CN)_6]^{4-}$ as redox probe, cTnI down to 1 pg mL^{-1} in human serum could be detected (Chekin et al., 2018) and others such a BNP (Grabowska et al., 2018).

Field-effect transistors (FETs) have drawn lately great consideration among the various electrical biosensor architectures due to their ability to directly record target biomolecule's interaction with the surface of the transducer into quantifiable electrical signals. The first demonstration of the detection of cTnT using silicon nanowires (SiNWs) based FETs goes back to 2009 (Chua et al., 2009) with a reported LOD of 1 fg mL^{-1}. Integration into microfluidic filtration chips, used to extract plasma directly from fingerpick blood samples, resulted in LOD of only 1 pg mL^{-1}. Even though the detection limit was decreased upon FET integration in a microfluidic flitration chip, the sensor has the advantage of reducing the sample dead volume and making the chip inexpensive. Conducting polymer nanowires have displayed great performance in label-fee diagnostics. The advantages of using conducting polymers as FET elements are biocompatibility and straightforward synthesis steps through chemical or electrochemical methods at ambient conditions. Change in electrical conductivity can be easily achieved by altering monomer, doping ratios, and oxidation states and process, offering exceptional potential for label-fee detection of cardiac biomarkers. One example is that of Lee et al. (2012) who reported on multiplexed sensing of cTnI, Myo, CK-MB and BNP using PANI nanowires with LOD of 250 fg mL^{-1} for cTnI and allowed sensing of CK-MB (150 fg mL^{-1}), BNP (50 fg mL^{-1}) and myoglobin (100 pg mL^{-1}).

A. Amperometric sensor for NT-proBNP and CRP

LOD: 470 pg ml^{-1}

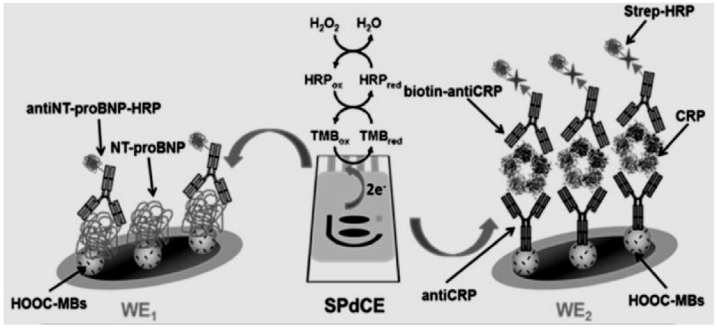

de Ávila et al. Electroanalysis 26 (2014) 254–26

B. Impedimetric sensor for cTnI and cTnT

LOD: 10 pg ml^{-1} (cTnI, cTnT)

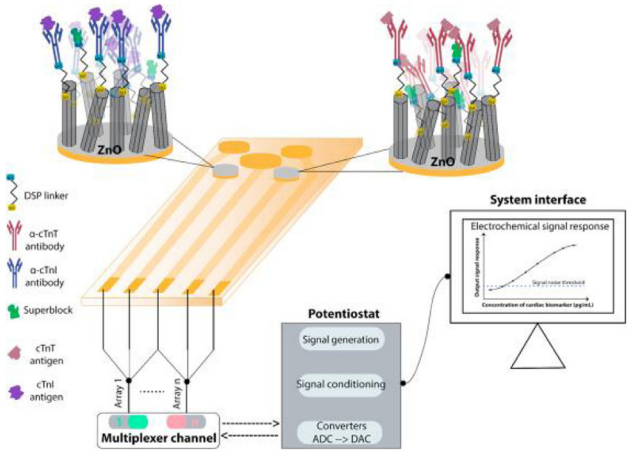

Shanmugama et al. Biosens. Bioelectron. **89 (2017)** 764.

C. Differential Pulse voltammetry (DPV)

LOD: 1 pg ml-1 (cTnT, BNP)

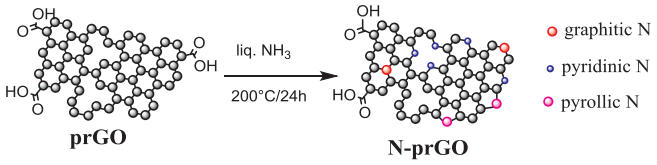

Chekin et al. Sens. Actuators B 262 (2018) 262, 180-187.

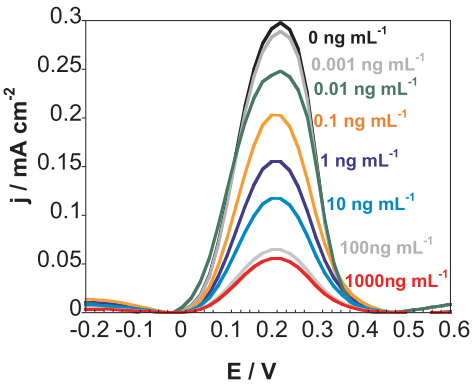

D. Field Effect Transistors (FET)

LOD: 1 pg ml^{-1} (cTnI)

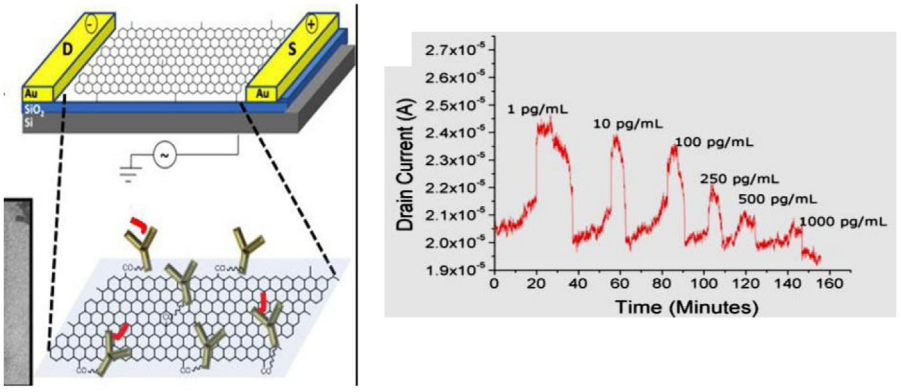

Tuteja et al, ACS Appl. Mater. Interfaces 6 (2014) 14767−14771.

Fig. 7. Electrochemical cardiac biomarkers sensors: (A) Development of a magneto-immunosensor for the simultaneous determination of NT-proBNP and CRP (reprint with permission from De Avila et al. (2014); (B) Label free impedimetric sensor based on ZnO decorated electrode array (reprint with permission from Shanmugam et al. (2017); (C) Formation of N-doped prGO for sensing of cTnI using DPV (reprint with permission from Chekin et al. (2018); (D) Schematic illustration of functionalized rebar graphene (f-RG) FET to detect cTnI and the dynamic response of the sensor (reprint with permission from Tuteja et al. (2014b).

Tuteja et al. (2014b) showed the interest of rebar graphene for integration with FET sensors for the detection of cTnI (Fig. 7**D**). Microwave-assisted unscrolling of carbon nanotubes was employed to form functionalized rebar graphene (f-RG), which was integrated onto an interdigitated electrode biochip in a FET configuration. Biofunctionalization with specific anti-cTnI antibodies allowed to design a sensor with required sensitivity.

One of the challenges in the field of electrochemical cardiac biomarkers sensing concerns sensitive recording in complex media other than human serum such as saliva or sweat where sub-picomolar (pM) detection limits are requested. Nanoparticles, nanowires, nanotubes and graphene based nanosheets are not only useful for signal amplification (Choi et al., 2010; Zhou et al., 2010; Ahammad et al., 2011; Bhalla et al., 2012; Zapp et al., 2014; Wang et al., 2016), but also to increase the accessible electrochemical surface area (Kim et al., 2016) and eventually the loading capacity with antibodies. In addition, they are expected to enhance electron transfer rates, which will result in improved detection limits. Ahammad et al. used gold nanoparticles

Table 4
Performance and detection methods of different electrochemical cardiac immunosensors.

Method	Limit of detection	Linear range	Comments	Reference
Myoglobin; cut-off level 70–200 ng mL^{-1}				
EIS	100 ng mL^{-1}	NA	Interdigitated electrodes	(Tweedie et al., 2006)
Faradaic	5 ng mL^{-1}	NA	NPs modified Fe graphite electrode	(Suprun et al., 2011)
Conductance	1.4 ng mL^{-1}	NA	Polyaniline NWs	(Qureshi et al., 2010)
EIS	15 ng mL^{-1}	NA	Mixed self-assembled monolayer	(Billah et al., 2008)
Potentiometric	1000 ng mL^{-1}	NA	Surface molecular imprinting	(Wang et al., 2008)
Amperometric	80 ng mL^{-1}	85–925 ng mL^{-1}	Indirect sandwich assay	(O'regan et al., 2002)
Troponin I; 0.01–0.1 ng mL^{-1}				
SWV	24 pg mL^{-1}	1–10000 pM	Ferrocene-modified silica nanoparticles as amplification; aptasensor	(Jo et al., 2015)
Potentiometric	1 ng mL^{-1}	1–100 ng mL^{-1}	ITO-AuNPs, cTnI-HRP as secondary antibody	(Ahammad et al., 2011)
EIS	1 pg mL^{-1}	NA	ZnO on flexible porous polyimide	(Shanmugam et al., 2016)
EIS	1 pg mL^{-1}	NA	Multiplexed	(Shanmugam et al., 2017)
CV	0.4 pg mL^{-1}	NA	AuNPs electrodeposited onto Au electrode	(Shan et al., 2014)
Square wave anodic stripping voltammetry	4 pg mL^{-1}	NA	Reporter peptide labeled with and Ru-containing compound Au NPs-PDMS composite microfluidic system CdTe and ZnSe QDs labeled secondary antibodies	(Zhou et al., 2010)
Capacitance	0.2 ng mL^{-1}	NA	Citrate-capped AuNPs electrodeposited onto Au electrode, coated with anti-cTnI	(Bhalla et al., 2012)
EIS, CV	0.2 ng mL^{-1}	0.25–1 and 5–100 ng mL^{-1}	Label free Vertically aligned Carbon nanofibers array	(Periyakaruppan et al., 2013)
FET	2 ng mL^{-1}	NA	SnO_2 nanobelt	(Cheng et al., 2011)
Amperometric	0.033 ng mL^{-1}	0.1–10 ng mL^{-1}	polyethyleneimine (PEI)/carboxylated CNTs sandwich using HRP as tracer	(Gomes et al., 2013)
FET	~1 pg mL^{-1}	NA	Functionalized rebar graphene monolayers	(Tuteja et al., 2014a)
FET	10 pg mL^{-1}	10–300 pg mL^{-1}	ZnO nanowires	(Munje et al., 2015)
Amperometric	0.05 ng mL^{-1}	0.05–3 ng mL^{-1}	AuNPs modified graphene nanocomposite Ferrocene-graphene used as amplification molecule	(Liu et al., 2016)
EIS	NA	1.0 pg mL^{-1} – 10 ng mL^{-1}	Pt NPs on graphene-MWCNT	(Singal et al., 2016)
Potentiometric	0.16 μg mL^{-1}	NA	Molecularly imprinted biomaterials on the surface of MWCNT	(Moreira et al., 2011)
DPV	0.027 nM	NA	MIP technology	(Zuo et al., 2016)
EIS, FET	1 pg mL^{-1}	NA	SiNWs chip	(Zhang et al., 2011)
EIS	2.4 pg mL^{-1}	NA	GCE modified with Au NPS	(Wang et al., 2016)
CV	0.2 ng mL^{-1}	0.1–10 ng mL^{-1}	Streptavidin-microsphere modified SPE	(Silva et al., 2010)
Capacitance	0.07 ng mL^{-1}	0.07–6.83 ng mL^{-1}	Metal-oxide Semiconductor compatible Si NWs	(De Vasconcelos et al., 2009)
SWV	0.076 ng mL^{-1}	0.1–0.9 ng mL^{-1}	AuNP-Si4Pic^{+}Cl^{-}	(Zapp et al., 2014)
EIS	0.07 ng mL^{-1}	0.1–10 ng mL^{-1}	GCE coated with porous GO	(Kazemi et al., 2016)
FET	0.7–0.8 pg mL^{-1}	100 ng mL^{-1} – 1 pg mL^{-1}	SWCNTs	(Sharma et al., 2016)
Resistance	< 0.1 pg mL^{-1}	NA	Graphene sheets biochip	(Tuteja et al., 2014b)
CV, LSV, EIS	0.01 ng mL^{-1}	0.01–1 ng mL^{-1}	Graphene-ABA	(Tuteja et al., 2015)
Conductance	0.092 ng mL^{-1}-46 ng mL^{-1}	0.092 ng mL^{-1}	SiNWs	(Kong et al., 2012)
Anodic stripping voltammetry	0.5 ng mL^{-1}	0.8–5.0 ng mL^{-1}	MCM-42 mesoporous material modified carbon paste electrode	(Guo et al., 2005)
Troponin T; 0.01–0.1 ng mL^{-1}				
FET	10 fg mL^{-1} (in buffer) 10 pg mL^{-1} (human serum)	NA	Nanofluidic diode structures	(Liu and Yobas, 2014)
DPV	0.0035 ng mL^{-1}	0.0025–0.5 ng mL^{-1}	Amino-functionalized CNTs	(Silva et al., 2013)
FET	1 fg mL^{-1} (in buffer) 30 fg mL^{-1} (in human serum)	NA	CMOS SiNWs arrays	(Chua et al., 2009)
C-reactive proteins (CRP): > 3 μg (high risk)				
CV	0.5 ng mL^{-1}	0.5–500 ng mL^{-1}	MWCNT modified screen printed carbon electrode NHRP-labeled anti CRP for sensing	(Buch and Rishpon, 2008)
EIS	0.1 ng mL^{-1}	0.1–20 ng mL^{-1}	Three-dimensional ordered macroporous (3DOM) gold film modified electrode	(Chen et al., 2008)
DPV	5.4 ng mL^{-1}	NA	Magnetic beads sandwich assay	(Centi et al., 2009)
EIS	0.0115 ng mL^{-1}	1.15 ng mL^{-1}	Label free	(Hennessey et al., 2009)
Capacitive	0.01 pg mL^{-1}	NA	Diamond like carbon electrode	(Lee et al., 2009)
Capacitance	25 ng mL^{-1}	25–800 ng mL^{-1}	Gold interdigitated electrodes	(Qureshi et al., 2010)
Faradaic	0.001 ng mL^{-1}	1 pg mL^{-1} – 1 μg mL^{-1}	Nanostructured polystyrene electrode	(Kunduru et al., 2010)
EIS	11 ng mL^{-1}	0.05–0.5 and 2.5–5 mg mL^{-1}	VACNFs	(Gupta et al., 2014a, 2014b)
Potentiometric	0.000001 ng mL^{-1}	0.00001 ng mL^{-1}-1 μg mL^{-1}	ZnO nanotubes	(Ibupoto et al., 2012)
Brain-type natriuretic peptide (BNP); cut-off level 0.1 ng mL^{-1}				
FET	100 fM	NA	Pt NPs decorated rGO	(Lei et al., 2017)
EIS	4 pg mL^{-1}	0.014–15 ng mL^{-1}	Peroxidase-labeled BNP antibodies on gold nanoparticle modified screen-printed carbon electrodes	(Serafin et al., 2018)
EIS	1 ag mL^{-1}.	NA	Silicon nanowells	(Prasad et al., 2013)

(*continued on next page*)

Table 4 (*continued*)

Method	Limit of detection	Linear range	Comments	Reference
Linear sweep voltammetry	10 ng mL^{-1}	NA	Acetylcholinesterase-labeled anti-BNP antibodies	(Matsuura et al., 2005a)
Linear sweep voltammetry	20–40 pg mL^{-1}	NA	Acetylcholinesterase-labeled anti-BNP antibodies with BNP; enzyme activity was measured on the basis of chemisorption/electrochemical desorption process of thiocholine, produced through the enzymatic reaction on a silver electrode.	(Matsuura et al., 2005a, 2005b)
N-terminal BNP (NT-proBNP); cut-off 0.25–2 ng mL-1				
Faradaic	0.006 ng mL^{-1}	NA	Nanostructured gold and carbon nanotubes composite	(Zhuo et al., 2011)
FET	100 fM	100 fM to 100 pM	AlGaN/GaN	(Chu et al., 2017)
Multianalyte sensing				
EIS	cTnI 1 pg mL^{-1} cTnT	NA	Multiplexed, flexible on ZnO nanostructures	(Shanmugam et al., 2017)
FET	cTnT MAB CK-MM CK-MB1 pg < : m < l	NA	Si NWS and filer chip	(Zhang et al., 2011)
FET	cTnT CK-MM CK-MB 100 fg mL^{-1}	NA	Si NWs cTnT CK-MM CK-MB	(Zhang et al., 2012)
EIS	CRP: 1 ng mL^{-1} MPO: 0.5 ng mL^{-1}	CRP: 10 ng mL^{-1} – 100 μg mL^{-1} MPO: 1 ng mL^{-1} – 1 μg mL^{-1}	Iridium oxide modified electrodes	(Venkatraman et al., 2009)
Faradaic	cTnI 0.01 ng mL^{-1} CRP 0.5 ng mL^{-1}	NA	Poly(dimethylsiloxane)-Au NPs	(Zhou et al., 2010)
EIS	NT-pro-BNP CRP 0.47 ng mL^{-1}	NA	Carbon-based screen-printed electrodes	(De Avila et al., 2014)
FET	Myo 100 pg mL^{-1} cTnI 250 fg mL^{-1} CK-MB 150 fg mL^{-1} BNP 50 fg mL^{-1}	NA	PANI NWs combined with micro-circulation	(Lee et al., 2012)

SWAST: square-wave anodic stripping voltammetry; PDMS: poly(dimethylsiloxane); PANI: polyaniline nanowires SWCNTs: single-walled carbon nanotubes; MIP: molecularly imprinted polymer, NA: not available.

anchored to ITO electrodes and modified with anti-cTnI for cTnI capture. Detection of the binding event was achieved by further interaction with HRP labeled anti-cTnI antibody to catalyze H_2O_2 reduction and used as a measure (Ahammad et al., 2011). An ultrasensitive label-free cTnI biosensor was proposed by Kim in 2016 and is based on a honeycomb-like structures of SiNW field effect crystal tubes. Under the FET operation mode, a LOD of 5 pg mL^{-1} was achieved mainly ascribed to the fact that the honeycomb-like structure of SiNWs has large effective area and offers more electron transfer channel with good electronic transport property (Kim et al., 2016). Lei et al. (2017) reported recently the successful detection of BNP using a PtNPs decorated rGO-FET sensor. Liu et al. proposed a simple method to prepare Au NPs modified graphene nanocomposite to detect cTnI. cTnI antibodies were immobilized to ferrocene-modified graphene, where ferrocene is used as a signal amplification molecule (Liu et al., 2016).

5. Cardiac biosensors: where are they on the market?

Several cardiac testing systems are on the market (Table 5). One of the first is the Troponin T rapid test (TROPT) using strips to detect cTnI. It is based on a sandwich ELISA technique that is sensitive to cTnT above 640 pg mL^{-1} only. Since 1997, the cTnT assays have been improved. A breakthrough came with the troponin-sensing device by Abbott and Roche, able to rule out AMI at the first blood draw. Different monoclonal antibody assays as well as immunological sandwich techniques are on the market detecting the CK-MB blood level spectrophotometrically. The only BNP sensor on the market is that of Abbott Point of Care with a detection limit of 15 pg mL^{-1}, being in addition in line with clinical demands.

6. Conclusion

As cardiac biomarkers continue to increase in importance, there will be withstand interest in their quantification for the next years. For cardiovascular diseases, several high-valuable biomarkers that are etiologically specific, reproducible, validated in multiple populations and implemented in clinical care are identified. Many of these biomarkers have serum concentration in the ng mL^{-1} to pg mL^{-1} range; yet in other body fluids, the protein concentrations can differ over several orders of magnitude, with high-abundant proteins such as globulin or coagulation factors (in the range of g mL^{-1}) often masking low-abundant protein biomarkers. This made their specific analysis challenging for a long time. Due to the enormous progress made in biosensor technology together with technological advancement allowing the incorporation of microfluidic separation channels, a large range of cardiac immunosensors have been proposed. Nanoparticles and nanomaterials based sensing strategies have led to sensors with improved sensitivity by several orders of magnitude, some of them being used for signal amplification, others for enhancing the surface area, promote electron transfer rate and improving the signal to noise ratio. The latter approach is rather appealing as it is a label-free strategy combing nanomaterials with cardiac surface ligands in a highly reproducible manner. In this review, we have summarized the current state of the art of cardiac biosensors with a special focus on electrochemical detection principles, due to their wide range of possibilities including multiplexing, development of implanted sensors, to mention some of them. Having outlined the current research and progress in the field achieved in the last years, what are the predicted future outcomes?

Graphene and its related materials, notably reduced graphene oxide and its derivatives have been more widely used in the last years for the construction of cardiac sensors (Tuteja et al., 2014a, 2014b; Chekin et al., 2018; Grabowska et al., 2018). Detection limits as low as

Table 5
Characteristics of some commercially available cardiac biomarker detection technologies.

Device	*Cardiac marker*	*Detection limit*	*Detection method*
Dimension Vista (Siemens, Munich, Germany)	cTnI	15 pg mL^{-1}	Chemiluminescence
TROPT (Heidelberg, Germany)	cTnT	0.64 ng mL^{-1}	Colorimetry
AQT90 (Radiometer)	cTnI	0.010–50 ng mL^{-1}	Fluorescence benchtop instrument
		0,0095 ng mL^{-1}	
Elecsys (Roche, Basel, Switzerland)	cTnT	0.005 ng mL^{-1}	Electrochemiluminescence
ACS:180 (Bayer, Leverkusen, Germany)	cTnI	0.15 ng mL^{-1}	Chemiluminescence
Cobas h232 (Roche Diagnostics Ltd)	CK-MB	1–40 ng mL^{-1}	Fluorescence
	Myoglobin	30–700 ng mL^{-1}	Handheld device
	cTnT	50–2000 pg mL^{-1}	
	NT-proBNP	60–9000 pg mL^{-1}	
i-STAT (Abbott Point of Care, Princeton, US)	cTnI	0.02 ng mL^{-1}	Electrochemical detection (amperometric)
	CK-MB	0.6 ng mL^{-1}	Handheld device
	BNP	15 pg mL^{-1}	
Cardiac Reader System (Roche)	CK-MB	1–40 ng mL^{-1}	Fluorescence
	Myoglobin	30–700 ng mL^{-1}	Benchtop
	NT-proBNP	0.060–3 ng mL^{-1}	POC
	cTnT	0.1–3 ng mL^{-1}	
Alpha Dx (First Medical Inc.)	cTnI	0.09 ng mL^{-1}	Fluorescence detection
	CK-MB	0.4 ng mL^{-1}	
	Myoglobin	7 ng mL^{-1}	
		180 ng mL^{-1}	
Evidence® Cardiac Panel	cTnI	0.27 ng mL^{-1}	Enhanced chemiluminescence
	CK-MB	1.5 ng mL^{-1}	
	Myoglobin	2.7 ng mL^{-1}	

0.1 pg mL^{-1} have been achieved in the case of cTnI, being far below the required sensitivity for measuring in human blood samples. Such sensors will open the possibility to screen cardiac biomarkers in saliva samples (Campuzano et al., 2017), which will facilitate diagnosis of acute myocardial infarctions and other heart diseases. Indeed, most of the diagnostic methods of cardiac diseases are based on blood biomarkers. It is, however, an invasive procedure too aggressive for certain patients.

Saliva sampling is simple and expected to be an attractive diagnostic fluid within the near future (Miller et al., 2014). It is highly useful for patients with difficulties in collecting blood (elderly people, diabetic people, neonates, etc). It increases the compliance of people who require frequent monitoring over the day or several days. It does not need special instruments or trained people and insures minimal risk of contamination among patients and healthcare personnel to blood-borne pathogens such as HIV and hepatitis. Some of us demonstrated lately that nitrogen-doped reduced graphene oxide modified electrodes covalently modified with Tro4 aptamers result in electrochemical sensors applicable for cardiac troponin I (cTnI) sensing in saliva samples. These sensors revealed that acute myocardial infarction diagnosed patients, the most immediately life threatening syndrome causing severe adverse cardiac events such as irreversible damage in the myocardium, have saliva cTnI levels as high as 675 pg mL^{-1} (Chekin et al., 2018).

While several cardiac biomarkers have been identified over the years, the search for others is a continuing process. Troponin I remains the most widely used biomarker for sensor development. Next to cTnI, B-type natriuretic peptide (BNP) and N-terminal pro-B-type natriuretic peptide (NT-pro-BNP) have been recognized as powerful cardiovascular biomarkers for acute heart failure (Maalouf and Bailey, 2016). In clinical practice, NT-pro-BNP detection is mostly performed as NT-pro-BNP has a circulation time of about 1–2 h, while that of BNP is only of 20 min. Nevertheless, BNP would be the more desirable biomarker for heart failure due to its fast release kinetics, rapid diffusion from injured tissue to blood. Circulating microRNA has been recently proposed by Sayed et al. as a potential biomarker for AMI (Sayed et al., 2013) and might be an additional ligand for biosensors next to antigens and aptamers. This study is under clinical trial.

Implanted biosensors offer additional advantages such as providing continuous data on the levels of a target analyte, enabling rapid modification of the treatment as well as earlier detection of threating disease states. They have additional benefits such as avoidance of much of the inconvenience, pain and time demands of drawing blood for periodic analysis. Subcutaneous biosensors with the sensor implanted in the subcutaneous tissue and a lead wire extending to an external monitoring display are developed for glucose monitoring. There is currently no equivalent for cardiovascular diseases. Indeed, drawbacks such as risk of infection, poor esthetic appeal and limited lifespan might limit their development. Vascular implanted biosensors might represent a better route for cardiac biomarker detection. The use of skin patches where the biomarkers can be detected on line in the sweat glands might be another viable approach for the future. In any of these cases, biofouling issues have to be overcome to make them a reliable approach.

CRediT authorship contribution statement

Sabine Szunerits: Conceptualization. **Vladyslav Mishyn:** Writing - review & editing. **Iwona Grabowska:** Writing - original draft. **Rabah Boukherroub:** Writing - review & editing.

Acknowledgements

Financial support from the Centre National de la Recherche Scientifique (CNRS), the University of Lille, the Hauts-de-France region, the CPER “Photonics for Society”, and the Agence Nationale de la Recherche (ANR) through FLAG-ERA JTC 2015-Graphtivity project are acknowledged.

Declaration of interests

The authors declare that they have no known competing financial interests or personal relationships that could have appeared to influence the work reported in this paper.

References

Acharya, A.P., Nafisi, pM, Gardner, A., Mackay, J.L., Kundu, K., Kumar, S., Murthy, N., 2013. Chem. Commun. Camb. 49, 10379–10381.
Ahammad, A.J.S., Choi, Y.H., Koh, K., Kim, J.H., Lee, J.J., Lee, M., 2011. Int. J. Electrochem. Sci. 6, 1906–1916.
Apple, F.S., Jesse, R.L., Newby, L.K., Wu, A.H.B., Christenson, R.H., Cannon, C.P., Francis, G., Morrow, D.A., Ravkilde, J., Storrow, A.B., Tang, W., Jaffe, A.S., Mair, J., Ordonez-Llanos, J., Pagani, F., Panteghini, M., Tate, J., Members, N.W.G., Members, N.C.,

Markers, I.C.S., 2007. Clin. Chem. 53, 547–551.
Ara, M.N., Hyodo, M., Ohga, N., Hida, K., Harashima, H., 2012. PLoS One 7, e50174.
Azevedo, A.M., Martins, V.C., Prazeres, D.M.F., Vojinović, V., Cabral, J.M.S., Fonseca, L.P., 2003. Biotechnol. Annu. Rev. 9, 199–247.
Bhalla, V., Carrara, S., Sharma, P., Nangia, Y., Suri, C.R., 2012. Sens. Actuators B Chem. 161, 761–768.
Billah, M., Hays, H.C.W., Millner, P.A., 2008. Microchim. Acta 160, 447–454.
Bruls, D.M., Evers, T.H., Kahlman, J.A.H., Van Lankvelt, P.J.W., Ovsyanko, M., Pelssers, E.G.M., Schleipen, J., De Theije, F.K., Verschuren, C.A., Van Der Wijk, T., Van Zon, J.B.A., Dittmer, W.U., Immink, A.H.J., Nieuwenhuis, J.H., Prins, M.W.J., 2009. Lab Chip 9, 3504–3510.
Bruno, J.G., Richarte, A.M., Phillips, T., 2014. Microchem. J. 115, 32–38.
Buch, M., Rishpon, J., 2008. Electroanalysis 20, 2592–2594.
Buckley, L.F., Abbate, A., 2018. Eur. Heart J. 39, 2063–2069.
Bunyakul, N., Baeumner, A.J., 2015. Sensors 15, 547–564.
Campuzano, S., Yanez-Sedeno, P., Pingarron, J.M., 2017. Trac-Trends Anal. Chem. 86, 14–24.
Centi, S., Sanmartin, L.B., Tombelli, S., Palchetti, I., Mascini, M., 2009. Electroanalysis 21, 1309–1315.
Chekin, F., Vasilescu, A., Jijie, R., Singh, S.K., Kurungot, S., Iancu, M., Badea, G., Boukherroub, R., Szunerits, S., 2018. Sens. Actuators B Chem. 262, 180–187.
Chen, X.J., Wang, Y.Y., Zhou, J.J., Yan, W., Li, X.H., Zhu, J.J., 2008. Anal. Chem. 80, 2133–2140.
Cheng, Y., Chen, K.S., Meyer, N.L., Yuan, J., Hirst, L.S., Chase, P.B., Xiong, P., 2011. Biosens. Bioelectron. 26, 4538–4544.
Choi, D.H., Lee, S.K., Oh, Y.K., Bae, B.W., Lee, S.D., Kim, S., Shin, Y.B., Kim, M.G., 2010. Biosens. Bioelectron. 25, 1999–2002.
Chon, H., Lee, S., Yoon, S.Y., Lee, E.K., Chang, S.I., Choo, J., 2014. Chem. Commun. 50, 1058–1060.
Chu, C.H., Sarangadharan, I., Regmi, A., Chen, Y.W., Hsu, C.P., Chang, W.H., Lee, G.Y., Chyi, J.I., Chen, C.C., Shiesh, S.C., Lee, G.B., Wang, Y.L., 2017. Sci. Rep. 7, 5256.
Chua, J.H., Chee, R.E., Agarwal, A., Wong, S.M., Zhang, G.J., 2009. Anal. Chem. 81, 6266–6271.
Colley, K.J., Wolfert, R.L., Cobble, M.E., 2011. EPMA J. 2, 27–38.
Danese, E., Montagnana, M., 2016. Ann. Transl. Med. 4, 194.
De Avila, B.E.F., Escamilla-Gomez, V., Lanzone, V., Campuzano, S., Pedrero, M., Compagnone, D., Pingarron, J.M., 2014. Electroanalysis 26, 254–261.
De Vasconcelos, E.A., Peres, N.G., Pereira, C.O., Da Silva, V.L., Da Silva, E.F., Dutra, R.F., 2009. Biosens. Bioelectron. 25, 870–876.
Dorraj, G.S., Rassaee, M.J., Latifi, A.M., Pishgoo, B., Tavallaei, M., 2015. J. Biotechnol. 208, 80–86.
Dutra, R.F., Kubota, L.T., 2007. Clin. Chim. Acta 376, 114–120.
Ference, B.A., Ginsberg, H.N., Graham, I., Ray, K.K., Packard, C.J., Bruckert, E., Hegele, R.A., Krauss, R.M., Raal, F.J., Schunkert, H., Watts, G.F., Boren, J., Fazio, S., Horton, J.D., Masana, L., Nicholls, S.J., Nordestgaard, B.G., Van De Sluis, B., Taskinen, M.R., Tokgozoglu, L., Landmesser, U., Laufs, U., Wiklund, O., Stock, J.K., Chapman, M.J., Catapano, A.L., 2017. Eur. Heart J. 38, 2459–2472.
Gomes, S.L.R., Dias, A., Silva, M.M.S., Silva, B.V.M., Dutra, R.F., 2013. Microchem. J. 109, 10–15.
Grabowska, I., Sharma, N., Vasilescu, A., Iancu, M., Badea, G., Boukherroub, R., Ogale, S., Szunerits, S., 2018. ACS Omega 3, 12010–12018.
Guo, H.S., He, N.Y., Ge, S.X., Yang, D., Zhang, J.N., 2005. Talanta 68, 61–66.
Gupta, R.K., Meyyappan, M., Koehne, J.E., 2014a. RCS Adv. 4, 22642–22650.
Gupta, R.K., Periyakaruppan, A., Meyyappan, M., Koehne, J.E., 2014b. Biosens. Bioelectron. 59, 112–119.
Hamm, C.W., Goldmann, B.U., Heeschen, C., Kreymann, G., Berger, J., Meinertz, T., 1997. N. Engl. J. Med. 337, 1648–1653.
Hennessey, H., Afara, N., Omanovic, S., Padjen, A.L., 2009. Anal. Chim. Acta 643, 45–53.
Horii, M., Matsumoto, T., Uemura, S., Sugawara, Y., Takitsume, A., Ueda, T., Nakagawa, H., Nishida, T., Soeda, T., Okayama, S., Somekawa, S., Ishigami, K., Takeda, Y., Kawata, H., Kawakami, R., Saito, Y., 2013. J. Cardiol. 61, 410–416.
Ibupoto, Z.H., Jamal, N., Khun, K., Willander, M., 2012. Sens. Actuators B 166–167, 809–814.
Jo, H., Gu, H., Jeon, W., Youn, H., Her, J., Kim, S.K., Lee, J., Shin, J.H., Ban, C., 2015. Anal. Chem. 87, 9869–9875.
Kaisti, M., 2017. Biosens. Bioelectron. 98, 437–448.
Kar, P., Pandey, A., Greer, J.J., Shankar, K., 2012. Lab Chip 12, 821–828.
Kazemi, S.H., Ghodsi, E., Abdollahi, S., Nadri, S., 2016. Mater. Sci. Eng. C 69, 447–452.
Kim, K., Park, C., Kwon, D., Kim, D., Meyyappan, M., Jeon, S., Lee, J.S., 2016. Biosens. Bioelectron. 77, 695–701.
Kong, T., Su, R.G., Zhang, B.B., Zhang, Q., Cheng, G.S., 2012. Biosens. Bioelectron. 34, 267–272.
Kunduru, V., Bothara, M., Grosch, J., Sengupta, S., Patra, P.K., Prasad, S., 2010. Nanomedicine 6, 642–650.
Ladue, J.S., Wroblewski, F., Karmen, A., 1954. Science 120, 497–499.
Lee, I., Luo, X., Huang, J., Cui, X.T., Yun, M., 2012. Biosensors 2, 205–220.
Lee, J., Noh, G.H., Pyun, J.C., 2009. BioChip J. 3, 287–292.
Lei, Y.M., Xiao, M.M., Li, Y.T., Xu, L., Zhang, H., Zhang, Z.Y., Zhang, G.J., 2017. Biosens. Bioelectron. 91, 1–7.
Lin, M.C., Nawarak, J., Chen, T.Y., Tsai, H.Y., Hsieh, J.F., Sinchaikul, S., Chen, S.T., 2009. Biomicrofluidics 3, 34101.
Liu, G.Z., Qi, M., Zhang, Y., Cao, C.M., Goldys, E.M., 2016. Anal. Chim. Acta 909, 1–8.
Liu, Y.F., Yobas, L., 2014. Nano Lett. 14, 6983–6990.
Liyanage, T., Sangha, A., Sardar, R., 2017. Analyst 142, 2442–2450.
Maalouf, R., Bailey, S., 2016. Heart Fail. Rev. 21, 567–578.
Masson, J.F., Obando, L., Beaudoin, S., Booksh, K., 2004. Sensitive and real-time fiber-optic-based surface plasmon resonance sensors for myoglobin and cardiac troponin I. Talanta 62 (5), 865–870. https://doi.org/10.1016/j.talanta.2003.09.032.
Matsuura, H., Sato, Y., Niwa, O., Mizutani, F., 2005a. Anal. Chem. 77, 4235–4240.
Matsuura, H., Sato, Y., Niwa, O., Mizutani, F., 2005b. Sens. Actuators B 108, 603–607.
Miller, C.S., Foley, J.D., Floriano, P.N., Christodoulides, N., Ebersole, J.L., Campbell, C.L., Bailey, A.L., Rose, B.G., Kinane, D.F., Novak, M.J., Mcdevitt, J.T., Ding, X., Kryscio, R.J., 2014. JDR Clin. Res. Suppl. 93, 72–79.
Moreira, F.T.C., Dutra, R.A.F., Noronha, J.P.C., Cunha, A.L., Sales, M.G.F., 2011. Biosens. Bioelectron. 28, 243–250.
Morrow, D.A., Cannon, C.P., Jesse, R.L., Newby, L.K., Ravkilde, J., Storrow, A.B., Wu, A.H.B., Christenson, R.H., Apple, F.S., Francis, G., Tang, W., Members, N.W.G., Members, N.C., 2007. Clin. Chem. 53, 552–574.
Munje, R.D., Jacobs, M., Muthukumar, S., Quadri, B., Shanmugam, N.R., Prasad, S., 2015. Anal. Methods 7, 10136–10144.
O'regan, T.M., O'riordan, L.J., Pravda, M., O'Sullivan, C.K., Guilbault, G.G., 2002. Anal. Chim. Acta 460, 141–150.
Otaki, Y., Watanabe, T., Kubota, I., 2017. Clin. Chim. Acta 474, 44–53.
Palazzuoli, A., Gallotta, M., Quatrini, I., Nuti, R., 2010. Vasc. Health Risk Manag. 6, 411–418.
Panteghini, M., 1995. Enzyme and muscle diseases. Curr. Opin. Rheumatol. 7, 469–474.
Pawula, M., Altintas, Z., Tothill, I.E., 2016. Talanta 146, 823–830.
Penttila, I., Penttila, K., Rantanen, T., 2000. Clin. Chem. Lab. Med. 38, 187–197.
Periyakaruppan, A., Gandhiraman, R.P., Meyyappan, M., Koehne, J.E., 2013. Anal. Chem. 85, 3858–3863.
Prasad, S., Selvam, A.P., Reddy, R.K., Love, A., 2013. JALA 18, 143–151.
Qureshi, A., Gurbuz, Y., Kallempudi, S., Niazi, J.H., 2010. Phys. Chem. Chem. Phys. 12, 9176–9182.
Sayed, A.S.M., Xia, K., Yang, T.L., Peng, J., 2013. Dis. Markers 561–566.
Serafin, V., Torrente-Rodriguez, R.M., Gonzalez-Cortes, A., De Frutos, P.G., Sabate, M., Campuzano, S., Yanez-Sedeno, P., Pingarron, J.M., 2018. Talanta 179, 131–138.
Shan, M., Li, M., Qiu, X.Y., Qi, H.L., Gao, Q., Zhang, C.X., 2014. Gold Bull. 47, 57–64.
Shanmugam, N.R., Muthukumar, S., Chaudhry, S., Anguiano, J., Prasad, S., 2017. Biosens. Bioelectron. 89, 764–772.
Shanmugam, N.R., Muthukumar, S., Prasad, S., 2016. Sci. Rep. 6, 33423.
Sharma, A., Han, C.H., Jang, J., 2016. Biosens. Bioelectron. 82, 78–84.
Silva, B.V.M., Cavalcanti, I.T., Mattos, A.B., Moura, P., Sotomayor, M.D.T., Dutra, R.F., 2010. Biosens. Bioelectron. 26, 1062–1067.
Silva, B.V.M., Cavalcanti, I.T., Silva, M.M.S., Dutra, R.F., 2013. Talanta 117, 431–437.
Singal, S., Srivastava, A.K., Gahtori, B., Rajesh, 2016. Microchim. Acta 183, 1375–1384.
Sinning, C., Schnabel, R., Peacock, W.F., Blankenberg, S., 2008. Congest. Heart Fail. 14, 46–48.
Suprun, E.V., Shilovskaya, A.L., Lisitsa, A.V., Bulko, T.V., Shumyantseva, V.V., Archakov, A.I., 2011. Electroanalysis 23, 1051–1057.
Tadepalli, S., Kuang, Z.F., Jiang, Q.S., Liu, K.K., Fisher, M.A., Morrissey, J.J., Kharasch, E.D., Slocik, J.M., Naik, R.R., Singamaneni, S., 2015. Sci. Rep. 5, 16206.
Tuteja, S.K., Kukkar, M., Suri, C.R., Paul, A.K., Deep, A., 2015. Biosens. Bioelectron. 66, 129–135.
Tuteja, S.K., Priyanka, Bhalla, V., Deep, A., Paul, A.K., Suri, C.R., 2014a. Anal. Chim. Acta 809, 148–154.
Tuteja, S.K., Sabherwal, P., Deep, A., Rastogi, R., Paul, A.K., Suri, C.R., 2014b. ACS Appl. Mater. Interfaces 6, 14767–14771.
Tweedie, M., Subramanian, R., Lemoine, P., Craig, I., Mcadams, E.T., Mclaughlin, J.A., Maccraith, B., Kent, N., Ieee, 2006. IEEE Eng. Med. Biol. Soc. 1, 4610–4614.
Venkatraman, V.L., Reddy, R.K., Zhang, F.Y., Evans, D., Ulrich, B., Prasad, S., 2009. Biosens. Bioelectron. 24, 3078–3083.
Wainstein, M.V., Mossmann, M., Araujo, G.N., Gonçalves, S.C., Gravina, G.L., Sangalli, M., Veadrigo, F., Matte, R., Reich, R., Costa, F.G., Andrades, M., Da Silva, A.M.V., Bertoluci, M.C., 2017. Diabetol. Metab. Syndr. 9 (67-67).
Wang, B., Jing, R., Qi, H.L., Gao, Q., Zhang, C.X., 2016. J. Electroanal. Chem. 781, 212–217.
Wang, Q., Liu, W., Xing, Y.Q., Yang, X.H., Wang, K.M., Jiang, R., Wang, P., Zhao, Q., 2014. Anal. Chem. 86, 6572–6579.
Wang, Y., Wu, J.J., Chen, Y.J., Xue, F., Teng, J., Cao, J.X., Lu, C.X., Chen, W., 2015. Microchim. Acta 182, 331–339.
Wang, Y.T., Zhou, Y.X., Sokolov, J., Rigas, B., Levon, K., Rafailovich, M., 2008. Biosens. Bioelectron. 24, 162–166.
Wu, B., Jiang, R., Wang, Q., Huang, J., Yang, X.H., Wang, K.M., Li, W.S., Chen, N.D., Li, Q., 2016. Chem. Commun. 52, 3568–3571.
Wu, W.Y., Bian, Z.P., Wang, W., Wang, W., Zhu, J.J., 2010. Sens. Actuators B 147, 298–303.
Zapp, E., Da Silva, P.S., Westphal, E., Gallardo, H., Spinelli, A., Vieira, I.C., 2014. Bioconjugate Chem. 25, 1638–1643.
Zhang, D., Huang, L., Liu, B., Ni, H., Sun, H., Su, E., Chen, H., Gu, Z., Shao, X., 2018a. Biosens. Bioelectron. 106, 204–211.
Zhang, G.J., Chai, K.T.C., Luo, H.Z.H., Huang, J.M., Tay, I.G.K., Lim, A.E.J., Je, M., 2012. Biosens. Bioelectron. 35, 218–223.
Zhang, G.J., Luo, Z.H.H., Huang, M.J., Ang, J.J., Kang, T.G., Ji, H.M., 2011. Biosens. Bioelectron. 28, 459–463.
Zhang, J., Lv, X.F., Feng, W., Li, X.Q., Li, K.J., Deng, Y.L., 2018b. Microchim. Acta 185, 364–372.
Zhou, F., Lu, M., Wang, W., Bian, Z.P., Zhang, J.R., Zhu, J.J., 2010. Clin. Chem. 56, 1701–1707.
Zhuo, Y., Yi, W.J., Lian, W.B., Yuan, R., Chai, Y.Q., Chen, A., Hu, C.M., 2011. Biosens. Bioelectron. 26, 2188–2193.
Zuo, J.J., Zhao, X.Y., Ju, X.C., Qiu, S., Hu, W.S., Fan, T., Zhang, J.K., 2016. Electroanalysis 28, 2044–2049.